Magnetisation reversal in anisotropy graded Co/Pd multilayers

C. W. Barton[1, a)] and T. Thomson[1].

[1] School of Computer Science, The University of Manchester, Oxford Rd, Manchester, M13 9PL, UK.

We demonstrate high precision controllability of the magnetization reversal nucleation process in $[Co/Pd]_8$ multilayer films consisting of two sets of bilayers with high and low perpendicular anisotropy respectively. The anisotropy of the entire film is set by the degree of Co/Pd interfacial mixing during deposition which provides fine control of the anisotropy of an individual bilayer in the multilayer stack. The relative number of each type of bilayer is used to select the magnetisation reversal behavior such that changing one bilayer changes the properties of the entire multilayer through anisotropy averaging. A simple extension to the sputtering protocol would provide multilayer films with fully graded anisotropy while maintaining a constant saturation magnetization opening new possibilities for the creation of highly engineered multilayer structures for spin torque devices and future magnetic recording media.

1. Introduction

The magnetisation reversal properties of perpendicular magnetic anisotropy materials (PMA), such as Co/Pd multilayer thin films[1,2], are important for future nanoscale technologies such as bit patterned media (BPM) recording[3,4] and spin-torque transfer (STT) devices[5,6,7].

The reversal behavior of magnetic thin films with perpendicular anisotropy has been studied extensively[8] and it is widely accepted that the reversal mechanism is one dominated by nucleation followed by rapid domain-wall motion[9]. Reversal is nucleated at regions of low anisotropy which for materials of similar distributions of anisotropy means that the nucleation field is related to the average anisotropy in a consistent manner. The

reversal behavior of Co/Pd multilayers can be discussed in the context of the Mansuripur two-coercivity model where two extreme cases can be identified[10]. The first is when the energy barrier associated with nucleation is greater than the barrier for domain-wall pinning. The hysteresis loops that are characteristic of this behavior typically exhibit very sharp reversal transitions where domain-wall propagation is relatively unrestricted during magnetisation reversal[11]. The second extreme occurs when the energy barrier due to the nucleation is less than that for domain-wall pinning such that following nucleation domain-walls may become trapped by pinning sites requiring additional applied reverse field to complete magnetisation reversal and achieve saturation[12].

In this work we demonstrate controlled magnetisation reversal in Co/Pd multilayers by varying the nucleation field through precise tuning of the anisotropy in prototype graded anisotropy multilayers.

Creating the multilayers consisting of bilayers with two distinct anisotropies is achieved by using remote plasma sputtering[13] to disrupt the chemical integrity of the interfaces during the deposition process. This process allows us to tailor the anisotropy at the level of a single bilayer repeat[14] whilst crucially maintaining the crystallographic structure, microstructure and saturation magnetisation[15].

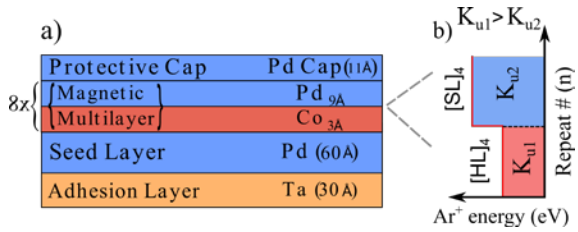

Fig 1: (Colour online) [(a)-(b)] schematic representation of the fabrication technique used to create two different anisotropy phases and nominal structure: (a) shows the nominal layer structure with the functionality of each layer labelled; and (b) shows an example for a film consisting of four repeats K_1 and four repeats K_2.

2. Experiment

Remote plasma sputtering was used to deposit Co/Pd multilayer structures where the nominal structure was Ta(30Å)/Pd(60Å)/[Co(3Å)/Pd(9Å)]$_8$/Pd(11Å), deposited on Si/SiO_2 substrates, at room temperature, as schematically shown in Fig. 1(a). The working pressure of Ar gas was $3x10^{-3}$ mBar, and the base pressure was < 9×10^{-9} mBar. During the deposition sequence the ion Ar^+ ion energy was increased at a specific point in the multilayer such that it was possible to set the anisotropy of the subsequently deposited layers through chemical intermixing of the interfaces. Schematically, this can be seen in Fig. 1(b) where the Ar^+ ion energy changes as a

function of the bilayer repeat number, at a specific bilayer. We introduce the notation that bilayers with a high perpendicular anisotropy are referred to hard layers (HL) whilst those with a low perpendicular anisotropy are referred soft layers (SL). In all the samples, the HL was deposited first followed by the SL. In the example shown, the schematic depicts a film where the first four bilayer repeats $[HL]_4$ are deposited at one specific Ar^+ ion energy, the subsequent four bilayers $[SL]_4$ are then deposited at a higher Ar^+ ion energy. In this work the two Ar^+ ion energies chosen were 200eV and 650eV which correspond to approximate uniaxial anisotropy values of $K_{u,1} = 3x10^6 ergs.cm^{-3}$ and $K_{u,2} = 1x10^6 ergs.cm^{-3}$ resulting in a 3:1 anisotropy ratio as measured on full film structures of a single K_u value.

The sample series investigated in this study comprised of 9 individually sputtered films. The value of the anisotropy constants was varied across the sample series such that the first sample comprised of eight bilayers deposited at one single Ar^+ ion energy $[HL]_8$. In subsequent samples, the Ar^+ ion energy was varied at a specific point in the film for example at the midpoint resulting the structure $[HL]_4/[SL]_4$. Finally arriving at the last sample comprised a single Ar^+ ion energy $[SL]_8$.

In order to characterise the films a number of experimental techniques were used. The structural properties were measured using X-ray diffraction (XRD) on a Phillips X'pert Pro diffractometer with CuK_α radiation. The magnetisation reversal properties and anisotropy values were measured using vibrating sample magnetometry (VSM) on a MicroSense model 10 vector VSM. The domain structure at remenance during magnetisation reversal was investigated using magnetic force microscopy (MFM) measured with a Veeco Dimension V scanning probe microscope.

3. Results and discussion.

Fig. 2 shows the normalized θ-2θ scans obtained by XRD in the Bragg-Brentano geometry. The samples

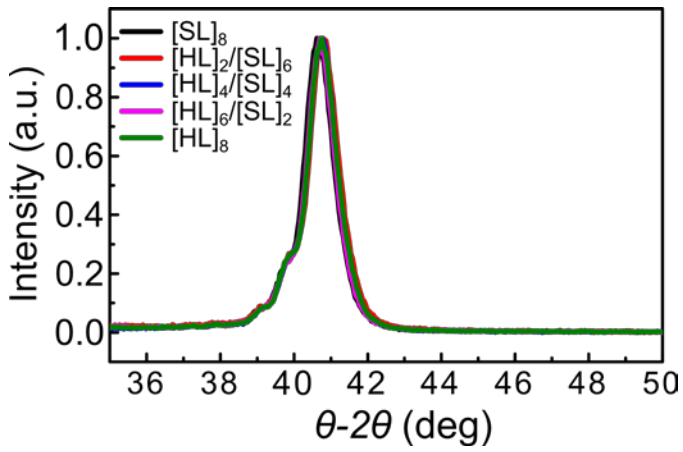

exhibit strong Co/Pd (111) texturing induced by the Ta/Pd seed layer structure[1]. The X-ray data are, within error, identical as the ratio of the two anisotropy layers (HL/SL) is varied across the series. This similarity suggests that the crystallographic structure and microstructure remain the same as the Ar^+ ion energy is varied. Additionally, Scherrer[16] analysis was performed on the Co/Pd (111) peak to assess the estimated grain size measured via perpendicular scattering. This was found to be consistently ≈7.83±0.02nm throughout the series and further demonstrates that the perpendicular grain size is insensitive to the Ar^+ ion energy as the ratio of the number of layers with different anisotropies is changed[14].

Fig. 3(a) shows the hysteresis loops obtained from VSM where the applied field (H_{app}) was perpendicular to the sample plane. The field sweep rate used during the measurement was approximately 500 $Oe.s^{-1}$ for field values corresponding to the reversal region and all measurements were undertaken at room temperature. It can be seen that the $[HL]_8$ film deposited at 200eV exhibits a very abrupt reversal behavior. This is in agreement with earlier work[14] where it was found that Co/Pd multilayer films with high anisotropy values exhibited very sharp magnetisation reversal transitions. Fig. 3(a) shows that the field at which the magnetisation reversal is initiated, reduces as more of the overall stack is comprised of [SL]'s deposited at 650 eV. In addition to the reduction of the nucleation field a broad tail is observed in the high field portion of the hysteresis curve. This broadening appears more prevalent the further the nucleation field is reduced. This systematic variation can be explained in more detail in the context of the Mansuripur two coercivity model[10].

As the number of SL bilayers in the films increases the nucleation field is reduced further. This is due to the reduced anisotropy of the magnetically softer region being exchange-coupled to the magnetically harder layers beneath resulting in anisotropy averaging through the thickness of the multilayer stack. This can be observed in

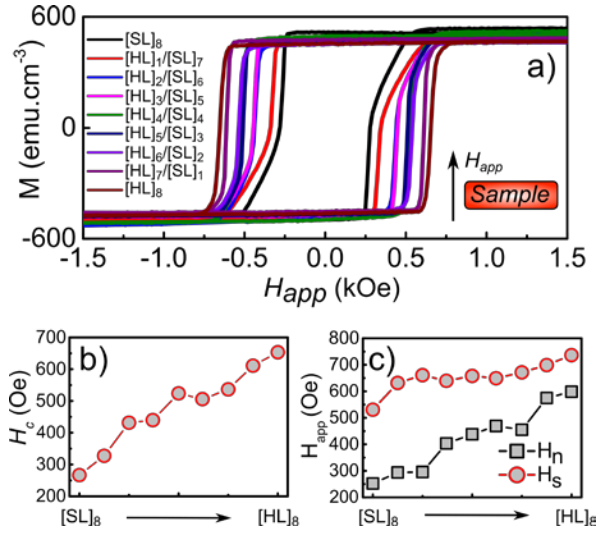

Fig 3: (Colour online) [(a)-(c)] (a) perpendicular magnetometry data obtained using VSM; (b) shows the extracted values for the coercivity as a function the film composition; and (c) shows the applied field H_{app} required for nucleation H_n and saturation H_s, calculated at 95% remanence and saturation respectively, as a function of film composition.

the perpendicular hysteresis loops which exhibit sharp transitions with little broadening of the tail in switching field distribution. This sharp reversal is due to the high energy barrier for nucleation of the HL bilayer. Fig.3(b) shows the values of coercivity (H_c) and fig.3(c) shows plots of the nucleation field H_n and the saturation field H_s as a function of total film structure. Here, H_n and H_s were measured as the applied field value at 95% remanence and saturation respectively. These data show that H_c is approximately equal to the nucleation field H_n and potentially allows H_c to be a useful parameter to characterise the nucleation field in these films. The systematic increase of H_n with number of HL bilayers shows that an averaging effect is present throughout the thickness of the film. This averaging is further demonstrated by the complete absence of a two-phase hysteresis loop which would be expected if the two types of bilayer nucleated independently.

To investigate the effect of varying the anisotropy within the multilayers in-plane magnetometry was performed. By applying an external magnetic in the plane of the sample it was possible to measure the uniaxial anisotropy K_u. Fig.4(a) shows the normalized in-plane magnetisation curves obtained by VSM. The data show how the

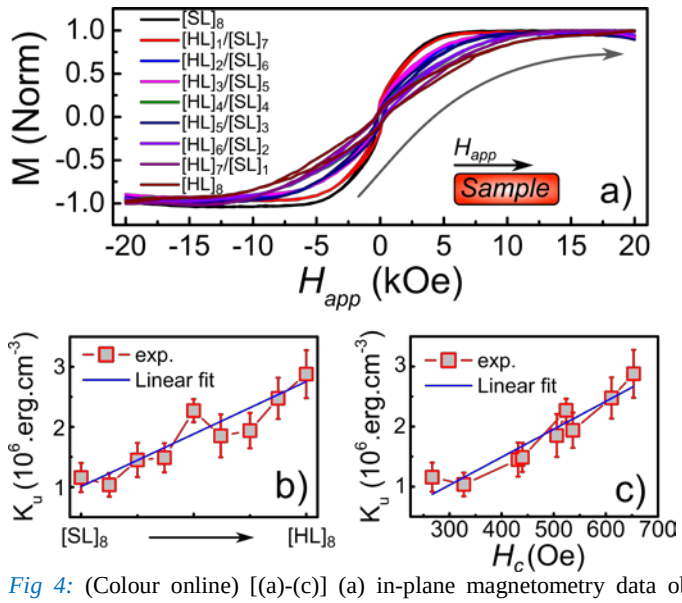

Fig 4: (Colour online) [(a)-(c)] (a) in-plane magnetometry data obtained using VSM show the normalized fourth quadrant data only; (b) the extracted values of the uniaxial anisotropy K_u as a function of the film composition; and (c)

magnetisation rotates into the plane of the sample with increasing applied field, from which it is possible to determine the average anisotropy field H_k [17]. Fig.4(b) shows the extracted uniaxial anisotropy K_u as a function of the ratio of the energies used to create the two anisotropy phases. It is shown that as the more of the film is comprised of the higher anisotropy phase [HL], the greater the average anisotropy. Fig.4(c) shows the relationship between H_c and the uniaxial anisotropy obtained from the in-plane magnetometry data and equation (1):

$H_k = 2K_u/M_s$. (1),

where M_s is the saturation magnetisation. Fig.4(c) demonstrates the correlation of the nucleation field and the anisotropy which scales linearly. These data provide further evidence of a vertical averaging of the magnetic properties within the HL and SL multilayer structure. This vertical averaging occurs such that as the relative ratio of the two anisotropies is varied, where a weighted average is observed. Furthermore the linear dependence shows how the nucleation field is determined by the fraction of HL bilayers in the stack.

The data show that the field at which magnetisation reversal saturates is nearly independent of the number of HL bilayers and only decreases when no HL is present, showing that the saturation process is governed by regions higher anisotropy.

The high field portion of the magnetisation reversal process is accompanied by a broadening of the switching field distribution as the coercivity and hence the nucleation field decreases with increasing number of SL bilayers. This is explained by the relationship between nucleation field and the total field (including the demagnetizing contribution) needed to induce domain wall motion. As the nucleation field is reduced, the effect of domain wall pinning becomes relatively stronger and we progressively measure a larger contribution of domain wall pinning to the total switching field distribution.

In order to quantitatively describe the relative contributions of the energy barriers associated with nucleation and domain-wall pinning a ratio of the areas of the switching field distribution (SFD) due to these two mechanisms was investigated. To define the ratio, the normalized SFD was analysed for each magnetization reversal curve. The distributions were then integrated independently such that, assuming a Gaussian distribution, the overlapping contribution due to the neighboring distribution was neglected from each area. Thus the ratio was defined as equation (2):

$$\frac{(sfd_2-\alpha_2)-(sfd_1-\alpha_1)}{(sfd_2+sfd_1)}, \qquad (2)$$

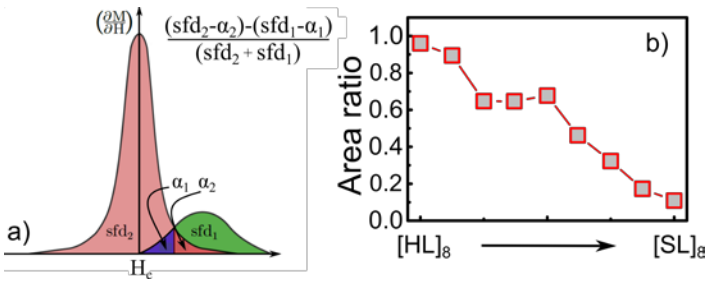

Fig 5: (Colour online) [a-b] (a) schematic representation of the ratio used to describe the relative contribution of nucleation and domain-wall pinning energy barriers; and (b) the defined switching field distribution area ratio as a function of the total film composition.

where sfd_x is the area of the Gaussian distribution associated with nucleation or domain-wall pinning and α_x is the area associated with the overlap of the distributions as shown in Fig.5(a). Fig.5(b) shows the ratio as a function of the relative portion of the two values of anisotropy starting from the film where the bilayers are $[HL]_8$ evolving to the film where all the bilayers are $[SL]_8$. These data demonstrate a monotonic decrease in the ratio as the sample series progresses. From the definition of the ratio a decrease is indicative of the increased presence in the switching field distribution due to domain-wall pinning. These data demonstrate that this process provides a very fine control over energy barriers for magnetisation reversal nucleation.

In order to investigate the magnetisation reversal further MFM was used to observe the magnetic domain structure, at remanence, during the reversal process. This was done by saturating the sample in one direction and subsequently applying a reverse field. The samples investigated in this study were selected to represent the two extreme cases, that is $[HL]_8$ and $[SL]_8$ respectively. Fig.6(a-d) shows the MFM sequence as a function of applied reverse field for the $[HL]_8$ sample. It is clear that following an initial nucleation event, a small increase in the applied reverse field results in rapid domain wall propagation. With a further increase of the applied field these domains expand rapidly until reverse saturation is reached. In these films with very sharp perpendicular hysteresis loops, magnetisation saturation is reached with little, if any, domain-wall pinning. In the film with

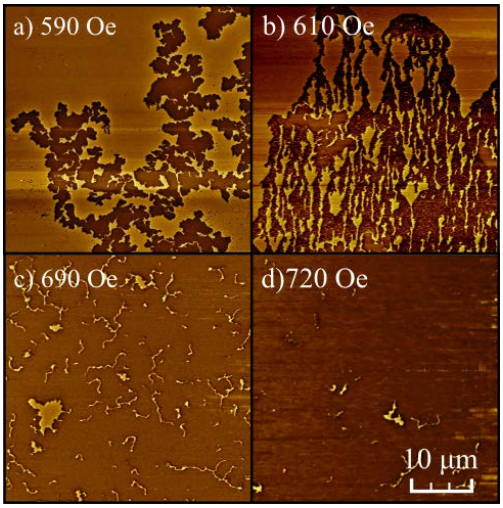

Fig 6: (Colour online) [(a)-(d)] MFM magnetisation reversal data for the $[HL]_8$ sample. Each micrograph represents a scan size of 40µm. The dark regions represent maagnetisations into-the-page and the light out-of-page, with an amplitude of ~500mdeg.

$[SL]_8$ the magnetisation reversal behavior is somewhat different. Here nucleation is initially followed by a rapid domain wall reversal process as shown in Fig.7(a-d). However, in this sample the domain-wall motion is impeded during the high field portion of the reversal process. This is seen by the change in the domain structure during the reversal process. Here the domain structure forms bubble-like domains that require an applied field greater than that needed for nucleation. With increasing applied field these bubble-like domains reduce in lateral

dimension until saturation is reached at a critical field[18] much larger than H_n. The observation of these small regions gives strong evidence for the existence domain wall annihilation and domain-wall pinning within the

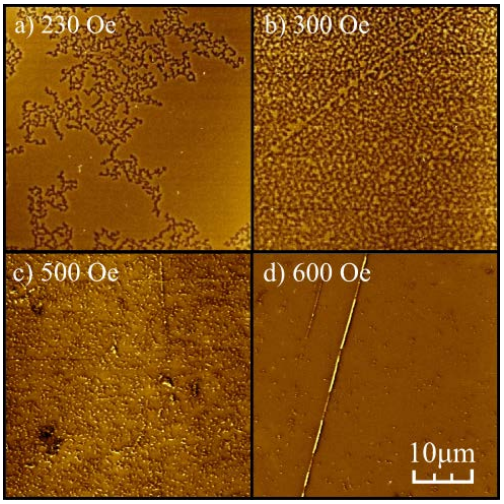

Fig 7: (Colour online) [(a)-(d)] MFM magnetisation reversal data for the $[SL]_8$ sample. Each micrograph represents a scan size of 40μm. The dark regions represent magnetisations into-the-page and the light out-of-page, with a phase amplitude of ~500mdeg.

films during reversal. This is such that that when the energy barrier associated with nucleation is controllably reduced, through anisotropy tuning, below the energy barriers associated with domain-wall pinning a change in the reversal process is observed. As this process occurs the shape of the hysteresis loops changes dramatically from sharp square loops to hysteresis loops where following an initial nucleation event domain-wall pinning and annihilation causes the trapping of domain walls.

4. Conclusions

In this work we have demonstrated that *in-situ* anisotropy tuning through interface modification using remote plasma sputtering is capable of producing a prototype graded anisotropy multilayer film. We show that systematically varying the film anisotropy of individual bilayers in HL/SL $[Co/Pd]_8$ multilayers, through varying the Ar^+ ion energy, during the deposition process, it is possible to tailor the nucleation of magnetization reversal. In-plane hysteresis loops demonstrate an effective vertical anisotropy averaging of the magnetic properties. This averaging, due to exchange coupling, results in a weighted average of the individual magnetic properties of each portion of the HL/SL film.

This work opens up the possibility of depositing multilayer structures where the uniaxial anisotropy K_u can be graded in such a way that optimum device parameters and characteristics can be achieved easily. Furthermore,

this work highlights the importance of high nucleation energy barriers needed for sharp magnetisation reversal behaviors, ideal for magnetic recording technologies.

Acknowledgements

The authors gratefully acknowledge the support of the UK EPSRC through grant number EP/G032440/1.

References

[1] J. M. Shaw, H. T. Nembach, T. J. Silva, S. E. Russek, R. Geiss, C. Jones, N. Clark, T. Leo, and D. J. Smith, Phys Rev B **80** (18), 184419 (2009).
[2] P. F. Carcia, J Appl Phys **63** (10), 5066 (1988).
[3] T. R. Albrecht, D. Bedau, E. Dobisz, H. Gao, M. Grobis, O. Hellwig, D. Kercher, J. Lille, E. Marinero, K. Patel, R. Ruiz, M. E. Schabes, L. Wan, D. Weller, and T. W. Wu, Ieee T Magn **49** (2), 773 (2013).
[4] O. Hellwig, E. E. Marinero, D. Kercher, T. Hennen, A. McCallum, E. Dobisz, T. W. Wu, J. Lille, T. Hirano, R. Ruiz, M. K. Grobis, D. Weller, and T. R. Albrecht, J Appl Phys **116** (12), 123913 (2014).
[5] J. Akerman, Science **308** (5721), 508 (2005).
[6] A. D. Kent, Nat Mater **9** (9), 699 (2010).
[7] T. N. A. Nguyen, Y. Fang, V. Fallahi, N. Benatmane, S. M. Mohseni, R. K. Dumas, and J. Akerman, Appl Phys Lett **98** (17), 172502 (2011).
[8] J. Pommier, P. Meyer, G. Penissard, J. Ferre, P. Bruno, and D. Renard, Phys Rev Lett **65** (16), 2054 (1990).
[9] S. Gadetsky, Ieee T Magn **31** (6), 3361 (1995).
[10] M. Mansuripur, J Appl Phys **63** (12), 5809 (1988).
[11] T. Thomson, K. OGrady, and G. Bayreuther, J Phys D Appl Phys **30** (11), 1577 (1997).
[12] D. M. Donnet, V. G. Lewis, J. N. Chapman, K. Ogrady, and H. W. Vankesteren, J Phys D Appl Phys **26** (10), 1741 (1993).
[13] M. Vopsaroiu, M. J. Thwaites, G. V. Fernandez, S. Lepadatu, and K. O'Grady, J Optoelectron Adv M **7** (5), 2713 (2005).
[14] C. W. Barton, T. J. A. Slater, R. M. Rowan-Robinson, S. J. Haigh, D. Atkinson, and T. Thomson, J Appl Phys **116** (20), 203903 (2014).
[15] T. Hauet, O. Hellwig, S. H. Park, C. Beigne, E. Dobisz, B. D. Terris, and D. Ravelosona, Appl Phys Lett **98** (17), 172506 (2011).
[16] U. Holzwarth and N. Gibson, Nat Nanotechnol **6** (9), 534 (2011).
[17] T. Thomson, B. Lengsfield, H. Do, and B. D. Terris, J Appl Phys **103** (7), 07F548 1 (2008).
[18] J. E. Davies, O. Hellwig, E. E. Fullerton, G. Denbeaux, J. B. Kortright, and K. Liu, Phys Rev B **70** (22) (2004).